SUPPORTING INFORMATION

Specific features of the spin density distribution and magnetic properties in a series of pyrazolyl-substituted nitronyl nitroxides: a magnetochemical and quantum chemical study

G.A. Letyagin,[a,b] P.A. Chernavin,[a,b] K.Yu. Maryunina,[a,b] S.E. Tolstikov,[a] E.V. Tretyakov,[c] G.V. Romanenko,[a] A.S. Bogomyakov[a,b]

[a] International Tomography Center SB RAS, 3A Institutskaya Street, Novosibirsk 630090, Russian Federation

[b] Novosibirsk State University, 1 Pirogova Street, Novosibirsk 630090, Russian Federation

[c] Zelinsky Institute of Organic Chemistry, Russian Academy of Sciences, 47 Leninsky Prosp., Moscow 119991, Russian Federation

Content

1. Synthesis

Commercial reagents NaH (60% dispersion in mineral oil, Sigma-Aldrich (USA)), 1,2-dibromoethane (99%, Dalhim (Russia)), 4-bromobut-1-ene (97%, Sigma-Aldrich (USA)), 1-bromo-2-methylpropane (99%, Sigma-Aldrich (USA)), 2-bromobutane (98%, Sigma-Aldrich (USA)) and solvents were used as received. Dimethylformamide (DMF) for synthesis was dried according to standard literature method [1]. 2-(1*H*-Pyrazol-4-yl)-4,4,5,5-tetramethyl-4,5-dihydro-1*H*-imidazole-3-oxide-1-oxyl (NN-4Pz^{H}) was synthesized according to the literature method [2]. The reactions were monitored by TLC using Macherey-Nagel «0.2 mm alumina N/UV254; plastic sheets». Column chromatography was carried out with the use of Al_2O_3 of chromatographic grade purchased from the Donetsk Plant of Chemical Reagents.

The microanalyses were performed on a «EURO EA3000» CHNS analyzer (HEKAtech, Webberg, Germany) at the Chemical Analytical Center of the Novosibirsk Institute of Organic Chemistry SB RAS. The IR spectra were recorded as KBr pellets on a Bruker Vector-22 spectrophotometer. Melting points were determined on an SMP3 (STUART), Cole-Parmer MP-800 (STUART) devices.

2-(1-(2-Bromoethyl)-1*H*-pyrazol-4-yl)-4,4,5,5-tetramethyl-4,5-dihydro-1*H*-imidazole-3-oxide-1-oxyl (NN-4Pz^{C2H4Br}). NaH (12 mg, 0.5 mmol) was added to NN-4Pz^{H} (0.1 g, 0.45 mmol) in 5 ml dry DMF and stirred for 15 min. Then 1,2-dibromoethane (0.85 g, 4.5 mmol) was added and stirred for 12 h. During the reaction, two more portions of NaH were added until the starting product disappeared (TLC control, Al_2O_3/ethyl acetate). The solvent was distilled off, the residue was chromatographed on a column with Al_2O_3 (2.5×20 cm), using $CHCl_3$ as an eluent. The first blue fraction containing the product with R_f = 0.73 was collected, evaporated and hexane was added to the residue. The resulting dark blue needle crystals were filtered and dried in air. Yield 0.1 g (67%), mp 103–104 ºC. IR spectrum, ν/cm^{-1}: 455, 488, 542, 565, 645, 671, 754, 853, 880, 946, 975, 1011, 1030, 1132, 1182, 1222, 1257, 1316, 1345, 1371, 1401, 1430, 1448, 1489, 1595, 1679, 2746, 2882, 2982, 3143. HRMS: *m/z* $[M]^+$ calcd. for $C_{12}H_{18}BrN_4O_2$: 329.0608; found: 329.0607.

2-(1-Vinyl-1*H*-pyrazol-4-yl)-4,4,5,5-tetramethyl-4,5-dihydro-1*H*-imidazole-3-oxide-1-oxyl (NN-4Pz^{vinyl}). A mixture of **NN-4Pz^{C2H4Br}** (0.25 g, 0.76 mmol), MeOH (5 ml) and KOH (43 mg, 0.76 mmol) was refluxed for 8 h until the starting compound completely disappeared (TLC control, Al_2O_3/ethyl acetate). The solvent was distilled off and residue was filtered through a layer of Al_2O_3 using benzene as a solvent. The filtrate was chromatographed on a column with SiO_2 (1.5x15 cm, benzene) using $CHCl_3$ as an eluent and collecting the first fraction of blue color. The eluate was evaporated, the residue was recrystallized from a mixture of CH_2Cl_2-*n*-

heptane. Yield 70 mg (37%), mp 76–79 ºC. IR spectrum, ν/cm^{-1}: 456, 537, 595, 621, 661, 673, 712, 753, 810, 844, 870, 905, 972, 985, 1012, 1022, 1128, 1181, 1213, 1311, 1341, 1373, 1403, 1432, 1450, 1484, 1599, 1656, 2933, 2988, 3076, 3112, 3147, 3445. Found (%): C, 57.6; H, 6.9; N, 22.2. $C_{12}H_{17}N_4O_2$. Calculated (%): C, 57.8; H, 6.9; N, 22.5.

2-(1-Allyl-1*H*-pyrazol-4-yl)-4,4,5,5-tetramethyl-4,5-dihydro-1*H*-imidazole-3-oxide-1-oxyl (NN-4Pz^{allyl}). NaH (72 mg, 3.00 mmol) was added portionwise to NN-4Pz^{H} (446 mg, 2.00 mmol) in 3.0 ml dry DMF and stirred for 15 min. Then 3-bromoprop-1-ene (290 mg, 2.40 mmol) was added and stirred for 1h until the starting NN-4Pz^{H} disappeared (TLC control, Al_2O_3/CH_2Cl_2). The solvent was distilled off, the residue was chromatographed on a column with Al_2O_3 (2.5×15 cm), using CH_2Cl_2 as an eluent. The first blue fraction containing the product with R_f~0.75 was collected, evaporated and hexane was added to the residue. The resulting dark blue needle crystals were filtered and dried in air. Yield 379 mg (77%), mp 103–104 ºC. IR spectrum, ν/cm^{-1}: 439, 465, 542, 596, 634, 661, 774, 816, 825, 857, 869, 949, 991, 1011, 1118, 1174, 1217, 1312, 1326, 1358, 1401, 1417, 1452, 1485, 1601, 1646, 2930, 2987, 3162, 3430.. Found (%): C, 59.5; H, 7.2; N, 21.3. Calculated for $C_{13}H_{19}N_4O_2$ (%): C, 59.3; H, 7.3; N, 21.3.

NN-4Pz^{Buen}, **NN-4Pz^{iBu}**, and **NN-4Pz^{secBu}** were prepared by a similar to **NN-4Pz^{allyl}** procedure using 4-bromobut-1-ene, 1-bromo-2-methylpropane and 2-bromobutane.

2-(1-(But-3-en-1-yl)-1*H*-pyrazol-4-yl)-4,4,5,5-tetramethyl-4,5-dihydro-1*H*-imidazole-3-oxide-1-oxyl (NN-4Pz^{Buen}). Yield 90%, mp 61–63 ºC. IR spectrum, ν/cm^{-1}: 438, 461, 541, 600, 645, 659, 753, 820, 878, 920, 941, 992, 1005, 1017, 1049, 1099, 1125, 1180, 1201, 1217, 1317, 1335, 1357, 1404, 1436, 1462, 1485, 1603, 1639, 2954, 2980, 2998, 3148, 3428.. Found (%): C, 60.5; H, 7.4; N, 20.1. Calculated for $C_{14}H_{21}N_4O_2$ (%): C, 60.6; H, 7.6; N, 20.0.

2-(1-Isobutyl-1*H*-pyrazol-4-yl)-4,4,5,5-tetramethyl-4,5-dihydro-1*H*-imidazole-3-oxide-1-oxyl (NN-4Pz^{iBu}). Yield 61%, mp 90–92 ºC. IR spectrum, ν/cm^{-1}: 481, 542, 617, 643, 666, 764, 826, 868, 946, 983, 1016, 1108, 1129, 1182, 1218, 1316, 1349, 1400, 1427, 1445, 1485, 1600, 2871, 2955, 3155, 3431. Found (%): C, 60.5; H, 8.5; N, 20.6. Calculated for $C_{14}H_{23}N_4O_2$ (%): C, 60.2; H, 8.3; N, 20.1.

2-(1-(*sec*-Butyl)-1*H*-pyrazol-4-yl)-4,4,5,5-tetramethyl-4,5-dihydro-1*H*-imidazole-3-oxide-1-oxyl (NN-4Pz^{secBu}). Yield 66%, mp 120–121 ˚C. IR spectrum, ν/cm^{-1}: 452, 541, 658, 752, 813, 868, 959, 976, 1016, 1123, 1182, 1219, 1309, 1341, 1371,1403, 1425, 1450, 1597, 2932, 2976, 3140, 3432. Found (%): C, 60.0; H, 8.5; N, 20.2. Calculated for $C_{14}H_{23}N_4O_2$ (%): C, 60.2; H, 8.3; N, 20.1.

2. X-Ray Crystallography

Table S1. Crystallographic Data and Experimental Details for NN-4Pz^{R}.

Compound	NN-4Pz^{C2H3} (vinyl)	NN-4Pz^{C2H4Br}	NN-4Pz^{nPr}	NN-4Pz^{C3H5} (allyl)	NN-4Pz^{C4H7} (buen)	NN-4Pz^{nBu}	NN-4Pz^{iBu}	NN-4Pz^{secBu}
FW	249.29	330.21	265.34	263.32	277.35	279.36	279.36	279.36
T, K	295	240	295	295	295	295	295	295
Space group, *Z*	*C*2/*c*, 16	*P*-1, 2	*Pbca,* 8	*Pbcn*, 8	$P2_1/c$, 4	$P2_1/n$, 4	$P2_1/n$, 4	$P2_1/c$, 4
a,	27.510(4)	6.4390(5)	11.2774(4)	11.4485(5)	12.2645(6)	13.9705(16)	7.5557(3)	7.3953(2)
b,	12.545(2)	11.1141(9)	13.9041(4)	16.5913(8)	11.4078(7)	7.5726(10)	21.6258(7)	12.4423(4)
c, Å	17.886(3)	11.5261(9)	18.6426(5)	14.7557(6)	12.3143(6)	15.0705(17)	9.6210(4)	17.4655(6)
α,	90	62.947(6)	90	90	90	90	90	90
β,	120.486(8)	76.883(6)	90	90	118.580(3)	93.979(9)	95.616(3)	98.508(2)
γ, °	90	89.549(5)	90	90	90	90	90	90
V, Å^3	5319.6(15)	711.10(10)	2923.20(15)	2802.8(2)	1512.97(14)	1590.5(3)	1564.51(10)	1589.39(9)
D_c, g cm^{-3}	1.245	1.542	1.206	1.248	1.218	1.167	1.186	1.167
θ_{max}, deg.	26.371	28.051	28.293	26.364	28.313	26.369	26.372	28.317
I_{hkl} (meas/uniq), R_{int}	22259 / 5422 0.0717	12442 / 3433 0.1039	18355 / 3618 0.0541	12742 / 2859 0.0434	14065 / 3769 0.0607	13434 / 3257 0.0694	13634 / 3194 0.0979	15241 / 3931 0.0608
I_{hkl} ($I>2\sigma_I$) / Ns	2399 / 428	1814 / 173	1750 / 178	1285 / 184	1810 / 245	1389 / 248	1311 / 188	1619 / 219
GooF	0.821	0.870	0.875	1.094	0.891	0.822	0.800	0.920
R_1 / wR_2 ($I>2\sigma_I$)	0.0449 / 0.0838	0.0471 / 0.0981	0.0405 / 0.0973	0.0480 / 0.1004	0.0468 / 0.1084	0.0395 / 0.0836	0.0481 / 0.0876	0.0599 / 0.1597
CCDC	2430089	2430092	2430095	2430090	2430091	2430094	2430093	2430096
Ref.	This work	This work	[3]	This work	This work	[4]	This work	[5]

3. Spin density delocalization details

Table S2. Mulliken spin populations (UB3LYP / def2-TZVP) on selected atoms of NN-4Pz^{R} radicals, selected bond lengths (Å) and {CN_2O_2}–Pz dihedral angles (º).

		NN-4Pz^{H} (α)	NN-4Pz^{H} (β)	NN-4Pz^{CD3}	NN-4Pz^{Et}	NN-4Pz^{C2D5}	NN-4Pz^{vinyl}	NN-4Pz^{C2H4Br}
	CCDC	NENNUP01	NENNUP02	BEMVOF01	WEHJOJ01	WEHJOJ	This work	This work
Pz	N(1)	-0.007	–0.006, –0.007	-0.008	-0.009	-0.008	-0.007	-0.008
	N(2)	0.005	0.005, 0.006	0.005	0.004	0.005	0.006	0.005
	C(3)	-0.024	–0.023, –0.022	-0.025	-0.022	–0.024	-0.021	-0.022
	C(4)	0.018	0.018	0.019	0.015	0.021	0.019	0.018
	C(5)	-0.041	–0.042, –0.041	-0.039	-0.037	–0.039	-0.041	-0.037
NN	C_{NN}	-0.173	–0.174	-0.176	-0.157	–0.176	-0.169	-0.178
	N_{NO}	0.257-0.265	0.257-0.274	0.265-0.267	0.260-0.266	0.261-0.266	0.261-0.266	0.264-0.266
	O_{NO}	0.335-0.342	0.335-0.337	0.328-0.348	0.32-0.344	0.332-0.346	0.328-0.345	0.326-0.351
	C_{Me}(eq)	<0.003	<0.002	<0.002	0.004	0.000	0.003	<0.001
	C_{Me}(ax)	0.02-0.022	0.017-0.019	0.019-0.020	0.015-0.018	0.019-0.020	0.017-0.018	0.020
	N–O	1.264(3)–1.297(3)	1.281(2)–1.295(2)	1.278(3), 1.282(2)	1.293(3), 1.294(3)	1.282(2), 1.287(2)	1.280(2)–1.288(2)	1.280(4), 1.290(2)
	C–$N_{\{NN\}}$	1.338(3)–1.353(4)	1.332(2)–1.353(2)	1.342(3), 1.347(2)	1.330(4), 1.336(3)	1.343(2), 1.344(3)	1.331(3)–1.350(3)	1.342(4), 1.353(3)
	{CN_2O_2}–Pz	2.7–9.9	10.2	3.4	5.1	8.6	4.0–5.8	5.9

Table S3. Mulliken spin populations (UB3LYP / def2-TZVP) on selected atoms of NN-4Pz^{R} radicals, selected bond lengths (Å) and {CN_2O_2}–Pz dihedral angles (º).

		NN-4Pz^{nPr}	NN-4Pz^{iPr}	NN-4Pz^{allyl}	NN-4Pz^{buen}	NN-4Pz^{nBu}	NN-4Pz^{iBu}	NN-4Pz^{secBu}
	CCDC	This work	REJPUS	This work	This work	This work	This work	This work
Pz	N(1)	-0.008	-0.008	-0.007	–0.007	–0.008	–0.007	–0.009
	N(2)	0.005	0.004	0.005	0.005	0.005	0.005	0.005
	C(3)	-0.024	-0.023	-0.024	–0.023	–0.025	–0.022	–0.024
	C(4)	0.017	0.015	0.017	0.015	0.017	0.017	0.019
	C(5)	-0.038	-0.036	-0.037	–0.038	–0.038	–0.035	–0.040
NN	C_{NN}	-0.170	-0.171	-0.171	–0.167	–0.169	–0.164	–0.171
	N_{NO}	0.264-0.267	0.261-0.274	0.264-0.265	0.262-0.268	0.259-0.275	0.262-0.266	0.262-0.268
	O_{NO}	0.326-0.345	0.324-0.345	0.328-0.343	0.330-0.337	0.332-0.335	0.323-0.342	0.325-0.347
	C_{Me}(eq)	<0.002	~0.003	<0.002	<0.003	<0.002	0.005-0.006	<0.001
	C_{Me}(ax)	0.018-0.019	0.017-0.020	0.019	0.017-0.018	0.018-0.021	0.015	0.019-0.020
	N–O	1.280(2), 1.285(2)	1.286(4), 1.291(4)	1.285(2), 1.286(2)	1.283(2), 1.284(2)	1.284(2), 1.287(2)	1.276(2), 1.285(2)	1.282(2), 1.283(2)
	C–$N_{\{NN\}}$	1.342(2), 1.343(2)	1.344(4), 1.351(5)	1.341(3), 1.344(3)	1.341(2), 1.344(3)	1.339(2), 1.349(2)	1.333(3), 1.337(3)	1.341(2), 1.347(2)
	{CN_2O_2}–Pz	8.8	2.7	0.5	3.0	2.2	7.8	5.8, 11.7*

* – minor conformation of disordered {Pz–*sec*Bu} fragment.

Table S4. Mulliken spin populations (UB3LYP / def2-TZVP) on selected atoms of NN-5Pz^{R} radicals, selected bond lengths (Å) and {CN_2O_2}–Pz dihedral angles (º)

		NN-5Pz^{H}	NN-5Pz^{Me}	NN-5Pz^{Et}	NN-5Pz^{nPr}	NN-5Pz^{nBu}
	CCDC	WEHJUP	HIKJEQ	KIQXAL	KIRBEU	KIQWUE
Pz	N(1)	-0.011	-0.009	–0.009	-0.010	-0.010
	N(2)	-0.037	-0.020	–0.023	-0.030	-0.023
	C(3)	0.016	0.008	0.009	0.013	0.010
	C(4)	-0.043	-0.025	–0.026	-0.036	-0.027
	C(5)	0.026	0.017	0.019	0.020	0.017
NN	C_{NN}	-0.164	-0.196	–0.193	-0.191	-0.191
	N_{NO}	0.261-0.264	0.257-0.258	0.255-0.260	0.258-0.267	0.254-0.262
	O_{NO}	0.311-0.357	0.330-0.362	0.327-0.365	0.33-0.362	0.322-0.369
	C_{Me}(eq)	0.006-0.010	0.000	0.000-0.001	<0.002	<0.002
	C_{Me}(ax)	0.011-0.013	0.018-0.019	0.018-0.019	0.017-0.019	0.017-0.019
	N–O	1.279(3)	1.278(2), 1.279(2)	1.280(2), 1.281(2)	1.277(1), 1.278(1)	1.272(1), 1.288(1)
	C–$N_{\{NN\}}$	1.325(3), 1.337(4)	1.340(2), 1.344(2)	1.340(2), 1.344(2)	1.349(2), 1.357(2)	1.338(2), 1.353(2)
	{CN_2O_2}–Pz	13.36	50.36	47.14	36.35	44.26

4. Magnetic properties, magnetic motif and quantum chemical calculations details

4.1 NN-4Pz^{R} radicals

4.1.1 Isolated radicals in the structures of NN-4Pz^{R} (R = butenyl)

For NN-4Pz^{butenyl}, no magnetically relevant contacts were revealed in the crystal structures according to the quantum chemical study – calculated J magnitudes are < 0.3 cm^{-1}. (Table S5). The effective magnetic moment μ_{eff} over the entire temperature range is close to a spin-only value of 1.73 μ_B for non-interacting monoradicals with S = 1/2 (Fig. S1). The $\mu_{eff}(T)$ dependences indicate the absence of meaningful exchange interactions. Magnetic susceptibility for NN-4Pz^{butenyl} obeys the Curie-Weiss law ($\chi = C/(T-\theta)$) with the best-fit parameter values C = 0.378±0.007 K·cm^3·mol^{-1} and θ = –1.25±0.02 K. The value of Weiss parameter θ indicates rather weak antiferromagnetic exchange interactions.

Table S5. Possible magnetically relevant contacts in the NN-4Pz^{butenyl} structure: intermolecular distances (Å) and calculated exchange coupling parameters (cm^{-1}).

	Type	Atom pair X…Y	Distance, Å	J_{calc}, cm^{-1}	Symmetry operator (if any)
1	NO…Me	O10…C7	3.861(3)	–0.23	Glide plain (*c*)
2	NO…Pz	O1…N15	3.974(1)	–0.14	Inversion
3	NO…Pz	O10…N14	3.889(1)	0.13	Screw axis 2_1

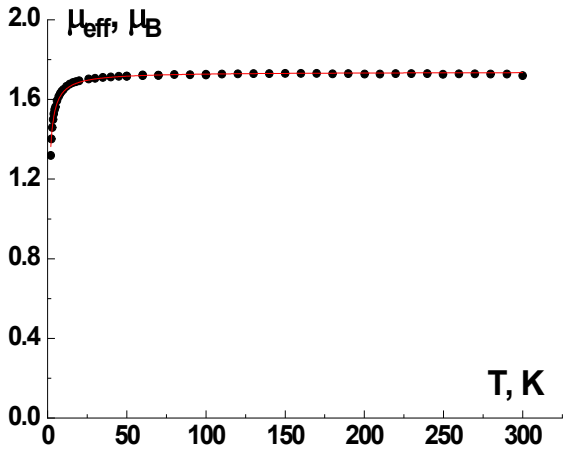

Fig. S1. $\mu_{eff}(T)$ dependence of NN-4Pz^{butenyl}. Fitting curve is shown as a red solid line.

4.1.2 Exchange-coupled dimers among the NN-4Pz^{R} radicals (R = CD_3, C_2D_5, C_2H_4Br, vinyl, iPr, nBu, secBu, H (α-polymorph))

In the structures of NN-4Pz^{R} (R = CD_3, C_2D_5, C_2H_4Br, vinyl, iPr, nBu, secBu, H (α)) radicals, exchange-coupled dimers were revealed. As it is shown in Figures S2-S7, contacts between spin-bearing atoms form different networks, *e.g.*, alternating chains. Quantum chemical analysis showed, that effective exchange interactions in all but one pair of radicals are rather small and may be neglected (Tables S6-S13 with the magnetically relevant contacts in bold). This reasoned the analysis of the $\mu_{eff}(T)$ dependence using the exchange-coupled dimer model (spin-Hamiltonian model $\hat{H} = -2J\hat{S}_1\hat{S}_2$) with the intercluster exchange interaction parameter zJ' taken into account (Fig. S8). In the case of NN-4Pz^{secBu}, the dimer model was selected due to the complexity of the "true" magnetic motif (Fig. S7) to avoid overparametrization. Best-fit values of J are in a good agreement with the results of quantum chemical study and listed in Table S4.

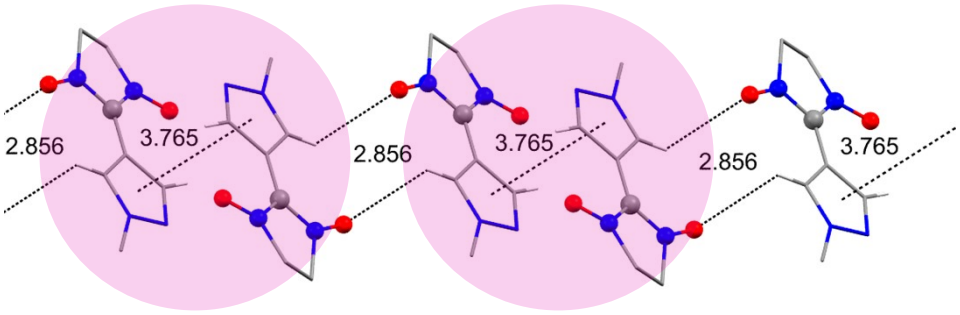

Fig. S2. Fragment of NN-4Pz^{CD3} crystal structure. Dimers of radical molecules connected by magnetically relevant Pz…Pz contacts are highlighted by purple ovals. The contacts are denoted under number 2 in Table S6.

Table S6. Possible magnetically relevant contacts in the NN-4Pz^{CD3} structure: intermolecular distances (Å) and calculated exchange coupling parameters (cm^{-1}). Hereinafter, selected magnetically relevant intermolecular contacts are highlighted in bold.

	Type	Atom pair X…Y	Distance, Å	J_{calc}, cm^{-1}	Symmetry operator (if any)
1	NO…Pz	O2…C11	3.517(2)	–0.36	Inversion
		O2…H14	2.86(2)		
2	**Pz…Pz**	**Pz centroids**	**3.765**	**–1.93**	**Inversion**
3	NO…Me	O1…C2	3.998(4)	0.00	Inversion
4	NO…Me	O2…C6	4.319(4)	0.00	Rotation axis 2

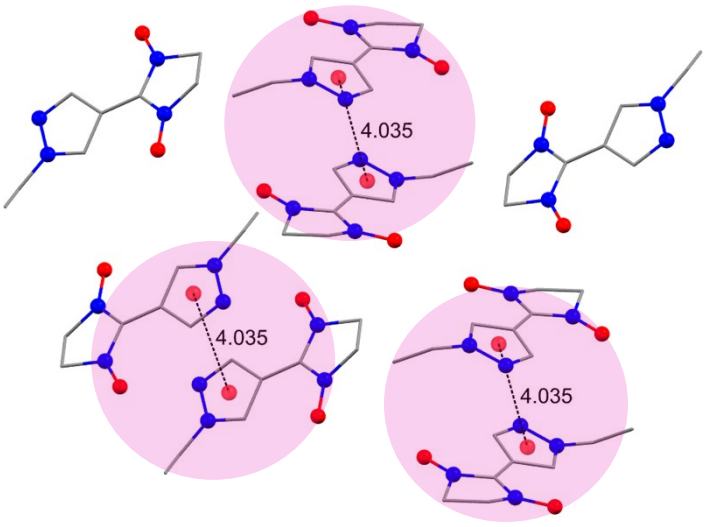

Fig. S3. Fragment of NN-4Pz^{C2D5} crystal structure. Dimers of radical molecules connected by magnetically relevant Pz…Pz contacts are highlighted by purple circles. The contacts are denoted under number 4 in Table S7.

Table S7. Possible magnetically relevant contacts in the NN-4Pz^{C2D5} structure: intermolecular distances (Å) and calculated exchange coupling parameters (cm^{-1}).

	Type	Atom pair X…Y	Distance, Å	J_{calc}, cm^{-1}	Symmetry operator (if any)
1	NO…Me	O1…C2	4.495(3)	0.25	Rotation axis 2
2	NO…NO	O2…O2	4.751(2)	–0.26	Inversion
	NO…Me	O2…C6	4.243(3)		
3	NO…Pz	O1…H14	3.13(2)	0.07	Inversion
		O1…C12	3.785(2)		
		O1…O1	4.710(2)		
4	**Pz…Pz**	**Centroids of Pz**	**4.035**	**–1.23**	**Inversion**

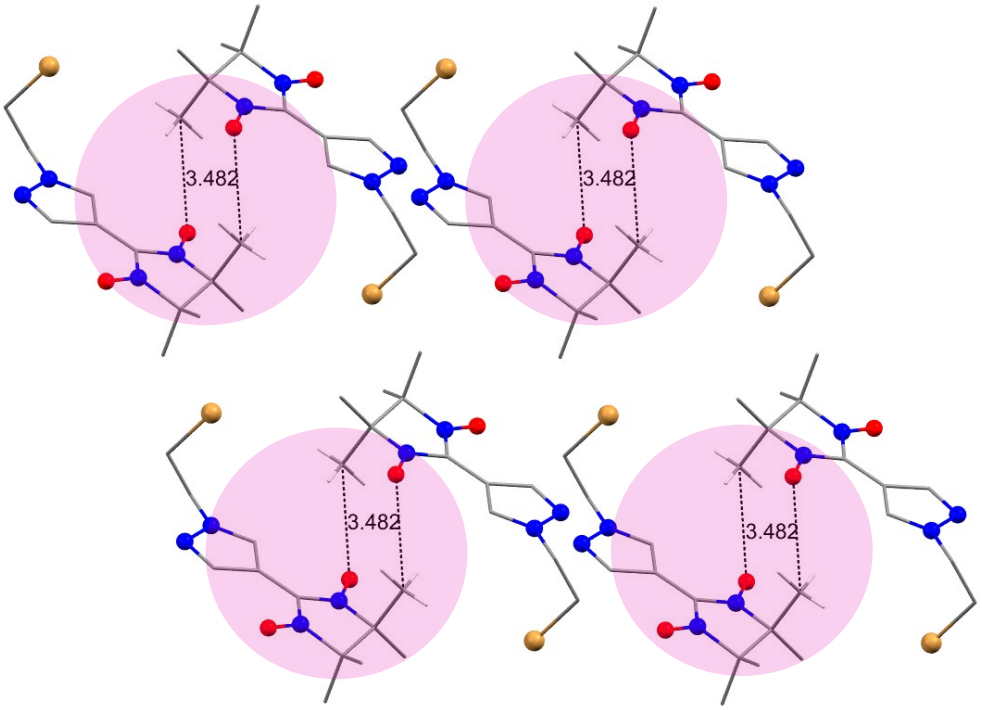

Fig. S4. Fragment of NN-4Pz^{C2H4Br} structure. Dimers of radical molecules connected by magnetically relevant NO…NO contacts are highlighted by purple circles. The contacts are denoted under number 1 in Table S8.

Table S8. Possible magnetically relevant contacts in the NN-4Pz^{C2H4Br} structure: intermolecular distances (Å) and calculated exchange coupling parameters (cm^{-1}).

	Type	Atom pair X…Y	Distance, Å	J_{calc}, cm^{-1}	Symmetry operator (if any)
1	**NO…Me**	**O2…C5**	**3.482(7)**	**1.05**	**Inversion**
2	NO…Me	O1…C3	3.78(1)	–0.11	Inversion
3	NO…Me	O2…C5	3.467(8)	–0.10	Translation [100] (along *a*)
4	NO…Pz	O2…H10	2.73(2)	–0.07	Inversion
		O2…C10	3.437(5)		
		O2…O2	3.974(5)		
5	Pz…Pz	O9…N4	3.572(9)	0.22	Inversion
		Pz centroids	5.089		
6	NO…Pz	O1…N3	3.808(5)	0.34	Translation [100] (along *a*)
		O1…Pz centroid	4.031		

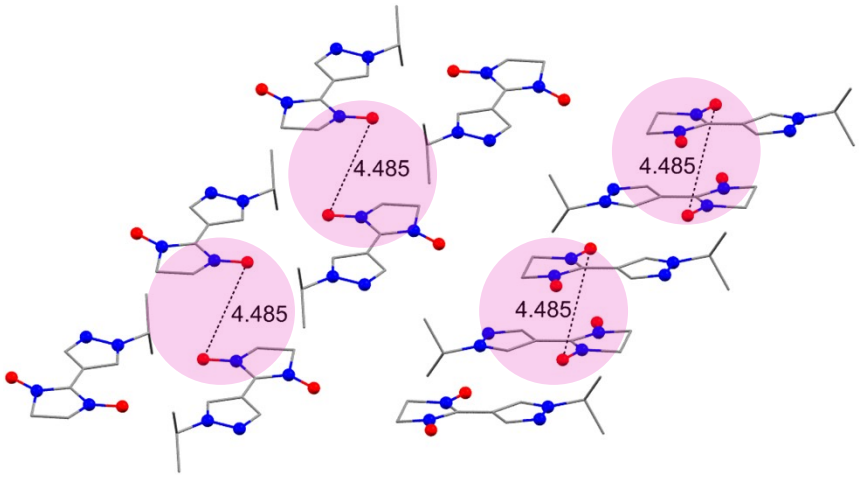

Fig. S5. Fragment of NN-4Pz^{iPr} crystal structure. Dimers of radical molecules connected by magnetically relevant NO…NO (O…N = 4.485(4) Å) contacts are highlighted by purple circles. The contacts are denoted under number 1 in Table S9.

Table S9. Possible magnetically relevant contacts in the NN-4Pz^{iPr} structure: intermolecular distances (Å) and calculated exchange coupling parameters (cm^{-1}).

	Type	Atom pair X…Y	Distance, Å	J_{calc}, cm^{-1}	Symmetry operator (if any)
1	**NO…NO**	**O1…O1**	**4.485(4)**	**–1.65**	**Inversion**
		O1…N1	**4.230(4)**		
2	NO…Pz	O1…H3	2.60(3)	0.59	Inversion
		O1…C7	3.395(5)		
3	Me…Pz	C13…C7	3.362(6)	0.44	Translation [100] (along *a*)
4	NO…Me	O2…C9	3.603(6)	0.34	Screw axis 2_1

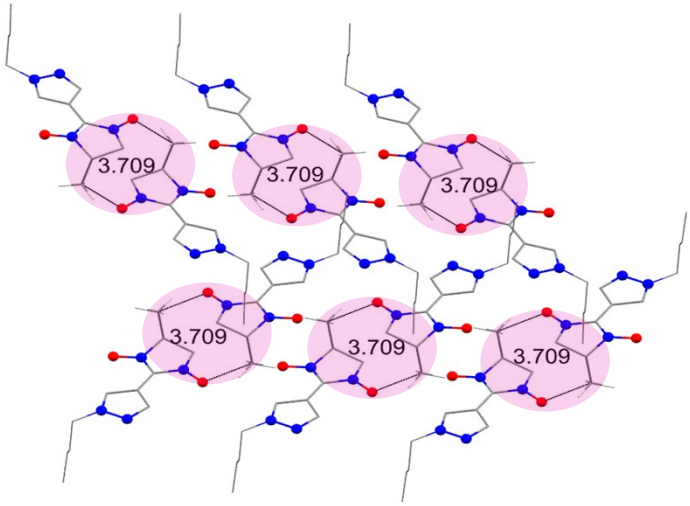

Fig. S6. Fragment of NN-4Pz^{nBu} crystal structure. Dimers of radical molecules connected by magnetically relevant NO…Me (O…C = 3.709(3) Å) contacts are highlighted by purple circles. The contacts are denoted under number 2 in Table S10.

Table S10. Possible magnetically relevant contacts in the NN-4Pz^{nBu} structure: intermolecular distances (Å) and calculated exchange coupling parameters (cm^{-1}).

	Type	Atom pair X…Y	Distance, Å	J_{calc}, cm^{-1}	Symmetry operator (if any)
1	NO…Me	O1…C7	3.523(3)	–0.36	Translation [010] (along *b*)
	NO…Pz	O10…C20	3.442(3)		
2	**NO…NO**	**O10…N9**	**4.517(2)**	**-1.01**	**Inversion**
	NO…Me	**O10…C5**	**3.709(3)**		
3	NO…Me	O1…C7	3.656(3)	0.30	Screw axis 2_1

Table S11. Possible magnetically relevant contacts in the NN-4Pz^{vinyl} structure: intermolecular distances (Å) and calculated exchange coupling parameters (cm^{-1}).

	Type	Atom pair X…Y	Distance, Å	J_{calc}, cm^{-1}	Symmetry operator (if any)
1	NO…Pz	O2B…C9B	3.686(4)	0.05	Inversion
		O2B… Pz centroid of molecule “B”	3.754		
2	NO…Pz	O1A…H10B	2.70(2)	0.77	Glide plain *c*
		O1A…C10B	3.436(2)		
		O1A…O1B	4.196(2)		
3	NO…Me	O2A…C2B	3.492(3)	–0.18	–
4	NO…Me	O2B…C2A	3.338(3)	–0.73	–
5	NO…Me	O1A…C6A	3.470(4)	0.70	Inversion
6	**NO…Pz**	**O2A…C9A**	**3.645(3)**	**–3.36**	**Rotation axis 2**
		O2A…Pz centroid of molecule “B”	**3.515**		

Table S12. Possible magnetically relevant contacts in the NN-4Pz^{H} (α) structure: intermolecular distances (Å) and calculated exchange coupling parameters (cm^{-1}).

	Type	Atom pair X…Y	Distance, Å	J_{calc}, cm^{-1}	Symmetry operator (if any)
1	NO…Me	O1A…C5B	3.500(4)	0.07	Inversion
2	NO…Me	O1B…C2A	4.659(6)	–0.39	-
3	NO…NO	O1A…O1B	4.138(3)	0.20	-
	NO…Me	O1A…C2B	4.651(4)		
4	NO…NPz	O2A…N3B	2.806(3)	0.31	-
5	NO…NO	O2B…O1B	3.648(3)	0.38	Translation [010] (along *b*)
	NO…CPz	O2B…C9B	3.188(3)		
	NO…Me	O1B…C5B	3.256(4)		
6	**Pz…Pz**	**Pz centroids (molecules "A")**	**3.725**	**–7.40**	**Inversion**
7	**Pz…Pz**	**„**	**3.772**	**–2.24**	**Inversion**

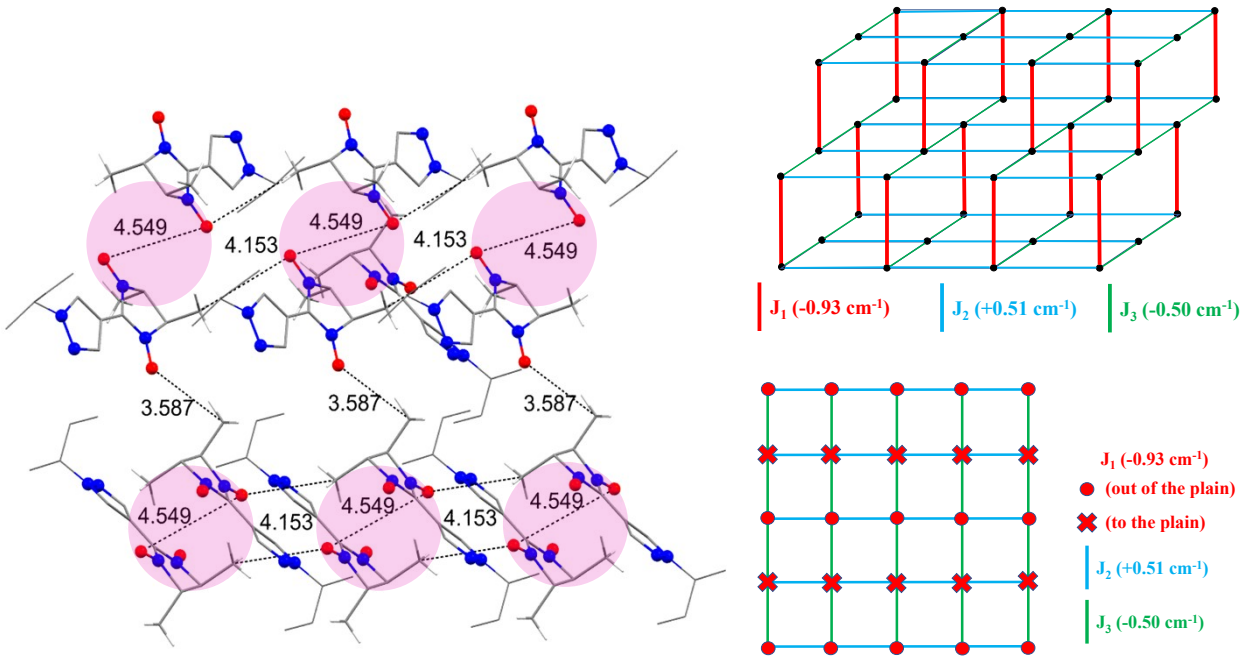

Fig. S7. Left: fragment of NN-4Pz^{secBu} crystal structure. Dimers of radical molecules connected by magnetically relevant NO…NO (O…O = 4.549(2) Å) contacts are highlighted by purple circles. The contacts are denoted under number 1 in Table S13. Right: "true" topology of 3D magnetic motif if contacts 2 and 3 from Table S13 are not neglected. Paramagnetic centers are shown as vertices with exchange interaction pathways shown as the edges of corresponding color; side view (top right) and from above – topology corresponds to the view of the crystal structure along the [100] (bottom right).

Table S13. Possible magnetically relevant contacts in the NN-4Pz^{secBu} structure: intermolecular distances (Å) and calculated exchange coupling parameters (cm^{-1}).

	Type	Atom pair X…Y	Distance, Å	J_{calc}, cm^{-1}	Symmetry operator (if any)
1	**NO…NO**	**O1…N2 (1)** **O1…O1 (1)**	**4.389(2)** **4.549(2)**	**–0.93**	**Inversion**
2	NO…Me	O1…C8	4.153(3)	0.51	Translation [100] (along *a*)
3	NO…Me	O10…C4	3.587(3)	–0.50	Screw axis 2_1
4	NO…NO	O1…O1 (2)	4.048(2)	0.08	Inversion

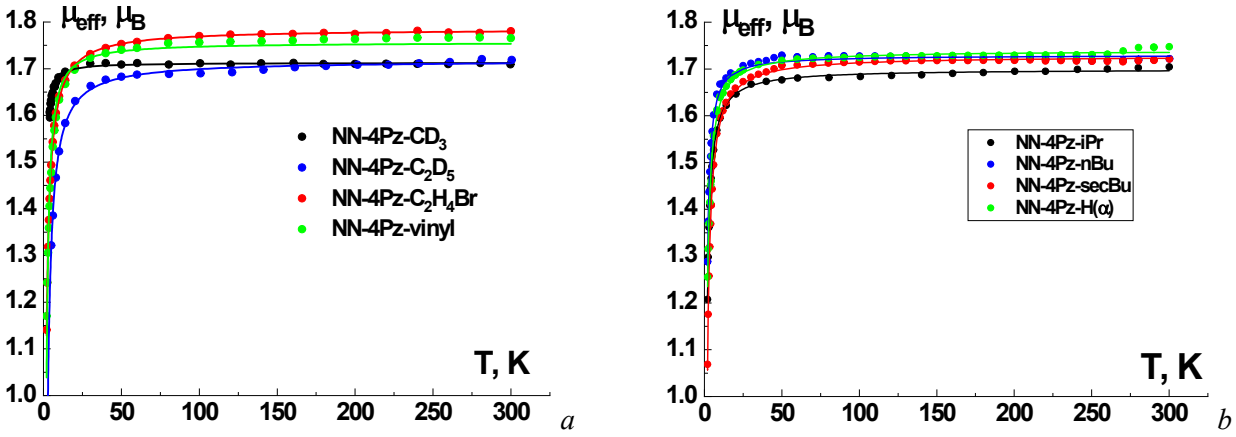

Fig. S8. $\mu_{eff}(T)$ dependence of NN-4Pz^{R} (*a*: R = CD_3 (●), C_2D_5 (●), C_2H_4Br (●), vinyl (●); *b*: R = iPr (●), nBu (●). secBu (●), H (α-polymorph) (●)). Fitting curves are shown as solid lines of the corresponding color.

4.1.3 Exchange-coupled tetramer among the NN-4Pz^{R} (R = H, β-polymorph) radicals

The analysis of the magnetic properties of NN-4Pz^{H} (β-polymorph) was described in the main text.

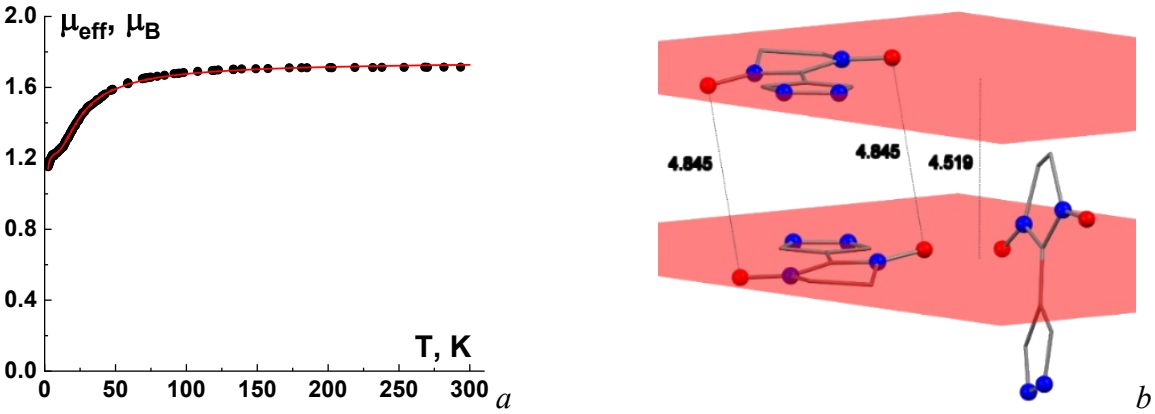

Fig. S9. *a*: $\mu_{eff}(T)$ dependence of NN-4Pz^{H} (β-polymorph). Fitting curve is shown as red solid line; *b*: Parallel arrangement of molecules in NN-4Pz^{H} (β) structure, with Pz…Pz plane-to-plane distance (4.519 Å) exceeding sum of Bondi radii (3.40 Å).

Table S14. Possible magnetically relevant contacts in the NN-4Pz^{H} (β) structure: intermolecular distances (Å) and calculated exchange coupling parameters (cm^{-1}).

	Type	Atom pair X…Y	Distance, Å	J_{calc}, cm^{-1}	Symmetry operator (if any)
1	NO…Me	O2…C19	3.384(2)	0.50	Glide plain *c*
2	NO…Me	O3…C8	3.527(2)	0.11	Screw axis 2_1
3	NO…Me	O3…C18	4.409(2)	0.00	Screw axis 2_1
4	**NO…NO**	**O1…O1**	**3.867(2)**	**–9.98**	**Inversion**
5	NO…NO	O2…O3	3.899(2)	0.50	Glide plain *c*
6	**NO…NO**	**O2…O4**	**3.230(2)**	**–3.07**	**-**
7	NO…NPz	O1…N4	2.704(2)	0.09	Screw axis 2_1
8	NO…NPz	O3…N8	2.812(2)	–0.14	Screw axis 2_1

4.1.4 Exchange-coupled chains among the NN-4Pz^{R} (R = Et, nPr, iBu) radicals

Quantum chemical investigation revealed that radical molecules form exchange-coupled chains in the structures of NN-4Pz^{Et}, NN-4Pz^{nPr} and NN-4Pz^{iBu} (Fig. S10-S12, Tables S15-S17). In the case of NN-4Pz^{Et} radical (Fig. S10), there are two alternating types of the short contacts (NO…Pz and NO…Me denoted as #1 and #2 in the Table S15). However, the calculated exchange interaction energies between the radicals are close enough (0.70 and 0.66 cm^{-1} for 1 and 2, respectively) to select the uniform exchange-coupled chain magnetic model (spin-Hamiltonian model $\hat{H} = -2J\sum_i \hat{S}_i\hat{S}_{i+1}$) with the z$J$' parameter included to analyze the experimental magnetic data as well as for NN-4Pz^{nPr} and NN-4Pz^{iBu}. Best-fit values of J obtained from the $\mu_{eff}(T)$ dependences (Fig. S13) analysis are in a good agreement with the calculated ones and listed in Table S4.

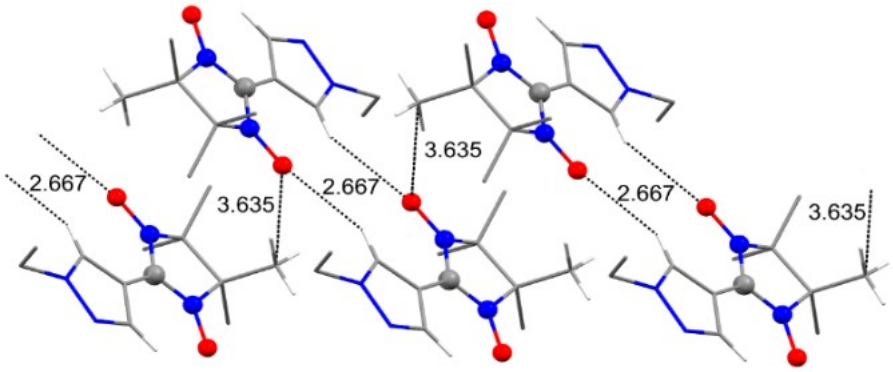

Fig. S10. Fragment of NN-4Pz^{Et} structure.

Table S15. Possible magnetically relevant contacts in the NN-4Pz^{Et} structure: intermolecular distances (Å) and calculated exchange coupling parameters (cm^{-1}).

	Type	Atom pair X…Y	Distance, Å	J_{calc}, cm^{-1}	Symmetry operator (if any)
1	**NO…Pz**	**O2…H19**	**2.667**	**0.70**	**Inversion**
		O2…C12	**3.440(4)**		
2	**NO…NO**	**O2…O2**	**4.631(3)**	**0.66**	**Inversion**
	NO…Me	**O2…C2**	**3.635(2)**		
3	NO…NO	O1…O1	3.545(4)	0.13	Inversion
	NO…Me	O1…C5	4.758(4)		

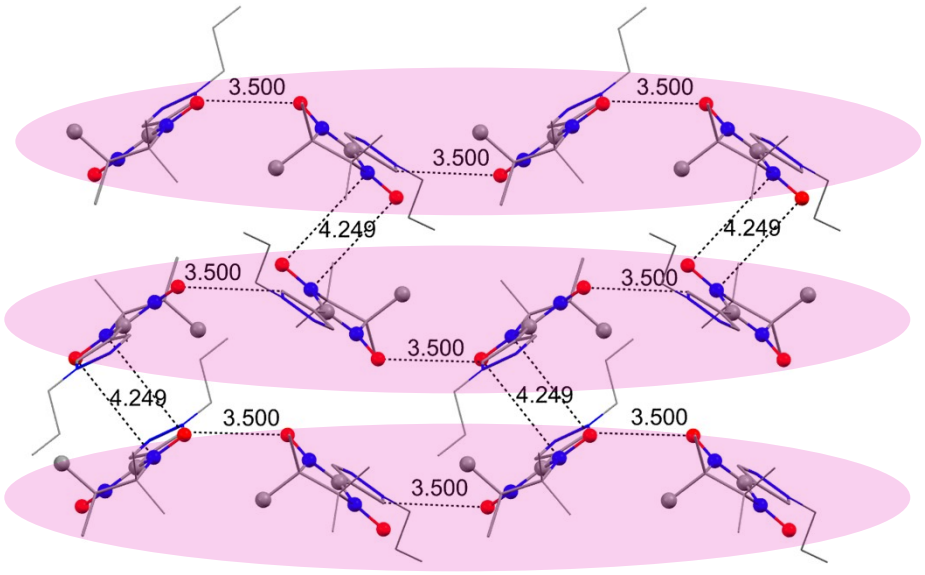

Fig. S11. Fragment of NN-4Pz^{nPr} structure. NO…Pz contacts (O…C = 3.500(2) Å) denoted under number 2 in Table S16 connect radical molecules into chains (highlighted by purple ovals).

Table S16. Magnetically relevant contacts in the NN-4Pz^{nPr} structure: intermolecular distances (Å) and calculated exchange coupling parameters (cm^{-1}).

	Type	Atom pair X…Y	Distance, Å	J_{calc}, cm^{-1}	Symmetry operator (if any)
1	NO…Me	O1…C8	3.634(2)	0.04	Inversion
2	**NO…Pz**	**O1…C19**	**3.500(2)**	**0.97**	**Glide plain *b***
	NO…Me	**O10…C4**	**3.570(2)**		
3	NO…NO	O10…N9	4.249(2)	-0.43	Inversion
	NO…Me	O10…C4	3.556(2)		

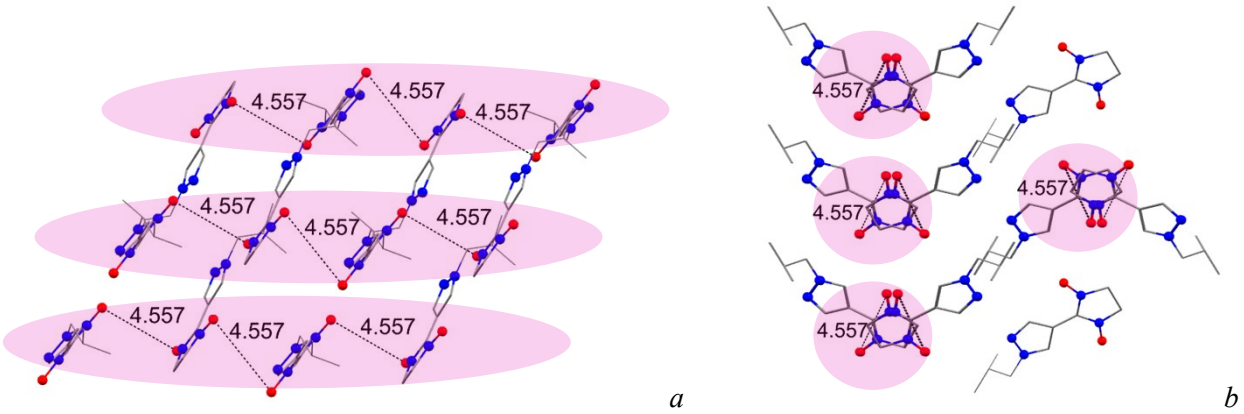

Fig. S12. Fragment of NN-4Pz^{iBu} crystal structure. NO…NO contacts (O…O = 4.557(3) Å) denoted under number 2 in Table S17 connect radical molecules into chains (highlighted in purple ovals). *a*: view along [100]; *b*: view along [001].

Table S17. Possible magnetically relevant contacts in the NN-4Pz^{iBu} structure: intermolecular distances (Å) and calculated exchange coupling parameters (cm^{-1}).

	Type	Atom pair X…Y	Distance, Å	J_{calc}, cm^{-1}	Symmetry operator (if any)
1	NO…NO	O1…O10 (1) O1…N9 (1)	4.037(2) 4.515(2)	–0.14	Translation [100] (along *a*)
2	**NO…NO**	**O1…O10 (2)** **O1…N9 (2)**	**4.557(3)** **4.421(3)**	**–0.68**	**Glide plain (*n*)**
3	NO…Me	O1…C8	3.825(3)	–0.13	Glide plain (*n*)

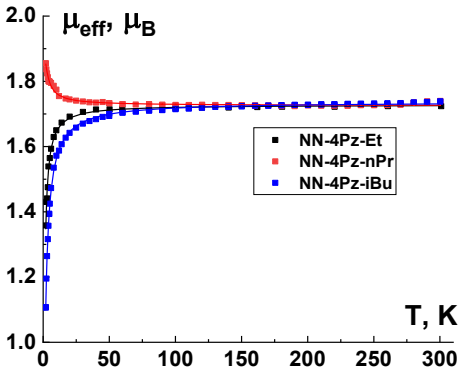

Fig. S13. $\mu_{eff}(T)$ dependences of NN-4Pz^{Et} (●), NN-4Pz^{nPr} (●) and NN-4Pz^{iBu} (●). Fitting curves are shown as solid lines of the corresponding color.

4.1.5 Exchange-coupled alternating chains among the NN-4Pz^{R} radicals (R = allyl)

The analysis of the magnetic properties of NN-4Pz^{allyl} was described in the main text.

Table S18. Possible magnetically relevant contacts in the NN-4Pz^{allyl} structure: intermolecular distances (Å) and calculated exchange coupling parameters (cm^{-1}).

	Type	Atom pair X…Y	Distance, Å	J_{calc}, cm^{-1}	Symmetry operator (if any)
1	**NO…NO**	**O10…N9**	**3.700(2)**	**–15.45**	**Rotation axis 2**
		O10…O10	**3.862(2)**		
	Pz…Pz	**Centroids Pz**	**3.803**		
2	NO…Me	O10…C7	3.925(3)	–0.13	Screw axis 2_1
3	**Pz…Pz**	**Centroids Pz**	**3.683**	**–1.92**	**Inversion**
4	NO…NO	O1…C7	4.990(3)	–0.04	Rotation axis 2

4.2 NN-5Pz^{R} radicals

4.2.1 Exchange-coupled dimers among the NN-5Pz^{R} radicals (R = Me, Et, nPr, nBu)

In the structure of NN-5Pz^{Me}, short contacts between spin-bearing atoms NO…Me (O…C = 3.169(5) Å) and NO…NO (O…O = 3.270(3) Å), denoted as #3 and #1 in Table S19, respectively, connect radical molecules into hexagonal net (Fig. S14). Analysis of the experimental $\mu_{eff}(T)$ dependence (Fig. 11) led to an overparametrization. Taking advantage of the fact that the calculated exchange interaction energy corresponding to contact 3 is five times smaller than that corresponding to contact 1, the exchange-coupled dimer model (spin-Hamiltonian $\hat{H} = -2J\hat{S}_1\hat{S}_2$) was used with the intercluster exchange interaction parameter z*J'*. In the case of NN-5Pz^{nPr} radical (Fig. S15), dimers of radical molecules are formed by magnetically relevant NO…NO contact (O…O = 3.313(2) Å, denoted as 1 in Table S21). As for NN-5Pz^{nBu}, radical pairs are connected by NO…Me contact (O…C = 3.684(2) Å, denoted as 1 in Table S22). The analysis of their $\mu_{eff}(T)$ dependences was carried out *via* exchange coupled dimer model (spin-Hamiltonian $\hat{H} = -2J\hat{S}_1\hat{S}_2$). Best-fit *J* parameters along with calculated ones are listed in Table 1.

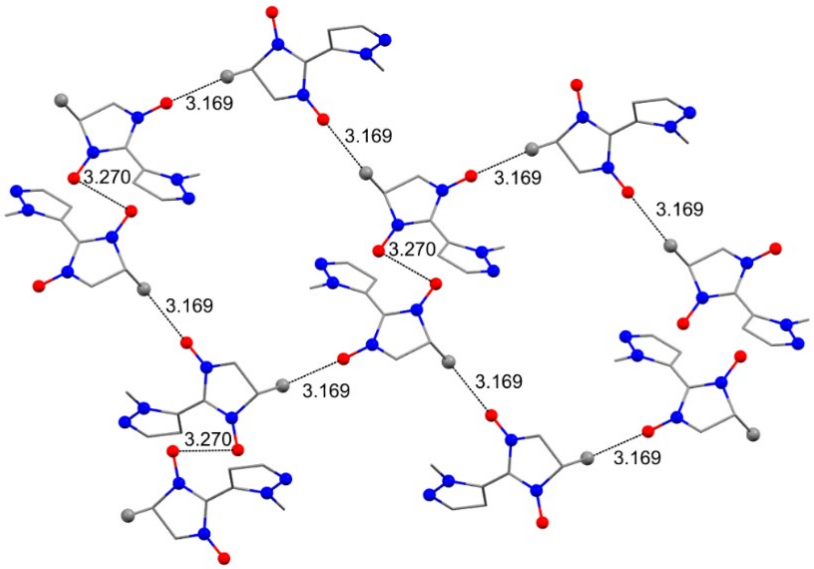

Fig. S14. Fragment of the NN-5Pz^{Me} crystal structure.

Table S19. Possible magnetically relevant contacts in the NN-5Pz^{Me} structure: intermolecular distances (Å) and calculated exchange coupling parameters (cm^{-1}).

	Type	Atom pair X…Y	Distance, Å	J_{calc}, cm^{-1}	Symmetry operator (if any)
1	**NO…NO**	**O2…O2**	**3.270(3)**	**–11.0**	**Inversion**
2	NO…Pz	O2…H13	2.48(3)	–0.22	Inversion
		O2…C9	3.293(4)		
	NO…NO	O2…O2	4.695(2)		
3	NO…Me	O1…C5	3.169(5)	–2.06	Glide plane *c*

The analysis of the magnetic properties of NN-5Pz^{Et} was described in the main text.

Table S20. Possible magnetically relevant contacts in the NN-5Pz^{Et} structure: intermolecular distances (Å) and calculated exchange coupling parameters (cm^{-1}).

	Type	Atom pair X…Y	Distance, Å	J_{calc}, cm^{-1}	Symmetry operator (if any)
1	NO…NO	O2…O2	3.462(2)	0.12	Inversion
2	**NO…NO**	**O1…O1**	**3.593(1)**	**–13.4**	**Inversion**
3	NO…Pz	O2…C9	3.368(2)	–0.39	Inversion
		O2…H9	2.56(1)		
	NO…NO	O2…O2	4.415(1)		
4	NO…Me	O1…C3	3.394(2)	–0.34	Inversion

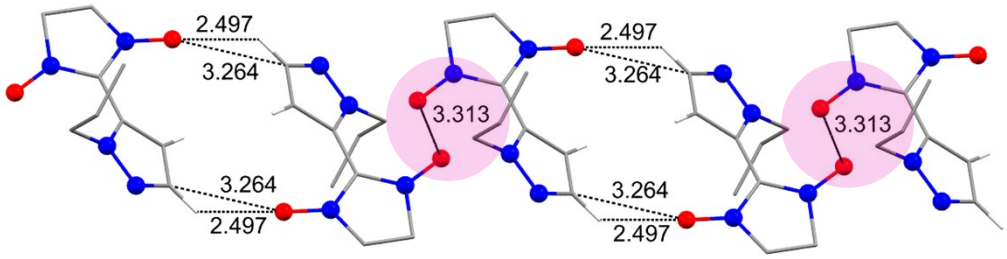

Fig. S15. Fragment of the NN-5Pz^{nPr} crystal structure. Exchange-coupled dimers of radical molecules are connected by NO…Me contacts (highlighted by purple circles; the contacts correspond to contact 1 in Table S21). Analysis of the $\mu_{eff}(T)$ dependence (Fig. 11) was performed using the exchange-coupled dimer model (spin-Hamiltonian model $\hat{H} = -2J\hat{S}_1\hat{S}_2$). The best-fit parameters are $J = –23.0±0.2$ cm^{-1}, g = 2.062±0.003.

Table S21. Possible magnetically relevant contacts in the NN-5Pz^{nPr} structure: intermolecular distances (Å) and calculated exchange coupling parameters (cm^{-1}).

	Type	Atom pair X…Y	Distance, Å	J_{calc}, cm^{-1}	Symmetry operator (if any)
1	**NO…NO**	**O1…O1**	**3.313(2)**	**–16.4**	**Inversion**
2	NO…NO	O1…O1	4.836(2)	0.00	Inversion
3	NO…Pz	O2…C9	3.264(2)	–0.69	Inversion
		O2…H9	2.50(2)		

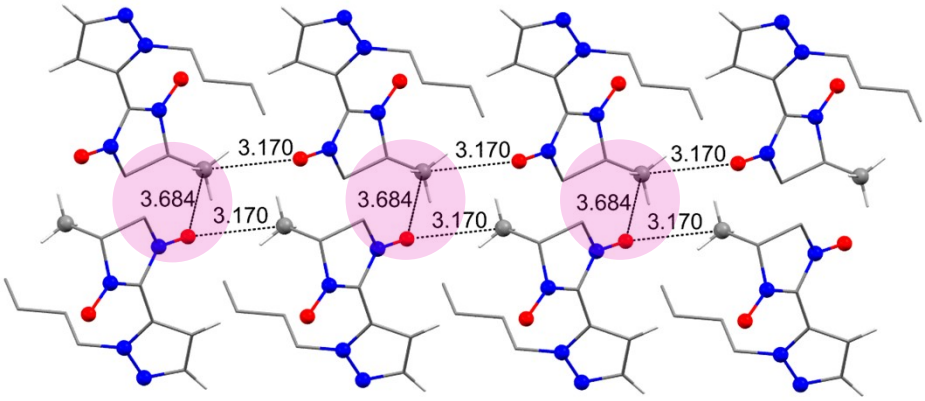

Fig. S16. Fragment of the NN-5Pz^{nBu} crystal structure. Exchange-coupled dimers of radical molecules are connected by NO…Me contacts (highlighted by purple circles; the contacts correspond to contact 1 in Table S22). Analysis of the $\mu_{eff}(T)$ dependence (Fig. 11) was performed using the exchange-coupled dimer model (spin-Hamiltonian model $\hat{H} = -2J\hat{S}_1\hat{S}_2$). The best-fit parameters are J = –0.98±0.02 cm^{-1}, g = 2.035±0.001.

Table S22. Possible magnetically relevant contacts in the NN-5Pz^{nBu} structure: intermolecular distances (Å) and calculated exchange coupling parameters (cm^{-1}).

	Type	Atom pair X…Y	Distance, Å	J_{calc}, cm^{-1}	Symmetry operator (if any)
1	**NO…Me**	**O10…C5**	**3.684(2)**	**–1.16**	**Inversion**
	NO…NO	**O10…O10**	**4.521(1)**		
2	NO…Me	O10…C5	3.170(2)	–0.09	Translatin [100] (along *a*)

4.2.2 Exchange-coupled alternating chains among the NN-5Pz^{R} radicals (R = H)

For NN-5Pz^{H} radical, alernating chains of molecules connected by contacts of two different types in the structure of NN-5Pz^{H} were revealed (Fig. S17, Table S23). Analysis of the $\mu_{eff}(T)$ dependence (Fig. 11) was performed using the exchange-coupled alternating chain model (spin-Hamiltonian model $\hat{H} = -2\sum_{i}(J_1\hat{S}_{2i}\hat{S}_{2i-1} + J_1\hat{S}_{2i}\hat{S}_{2i+1})$). The best-fit parameters are J_1 = –6.13±0.07 cm^{-1}, J_2 = –4.81±0.16 cm^{-1}; g = 1.901±0.003.). The sign of one calculated exchange interaction energy doesn't match with the experimental one (2.42 cm^{-1}).

Table S23. Possible magnetically relevant contacts in the NN-5Pz^{H} structure: intermolecular distances (Å) and calculated exchange coupling parameters (cm^{-1}).

	Type	Atom pair X…Y	Distance, Å	J_{calc}, cm^{-1}	Symmetry operator (if any)
1	NO…Pz	O2…H1	2.04(4)	2.42	Inversion
		O2…N2	2.902(4)		
	NO…NO	O2…O2	2.787(3)		
2	NO…NO	O1…O1	4.020(3)	–0.91	Rotation axis 2

5. Comparison of population analysis schemes

Since Mulliken formalism is known to be basis set dependent, we performed comparison of spin populations based DFT calculations with different basis sets: def2-SVP, def2-TZVP, def2-QZVP (Table S3) and compare Mulliken formalism with Löwdin formalism (Table S4) to validate our findings. Mulliken spin populations show much less pronounced variation upon basis set variation, compared to Löwdin ones. Moreover, Mulliken spin populations, calculated with def2-TZVP and def2-QZVP basis sets, show little to nothing difference (ca. 0.001 difference for Pz atoms). Finally, Löwdin spin populations demonstrate qualitatively the same trends upon variation substituent R as Mulliken ones (Fig S17, Tables S3, S4).

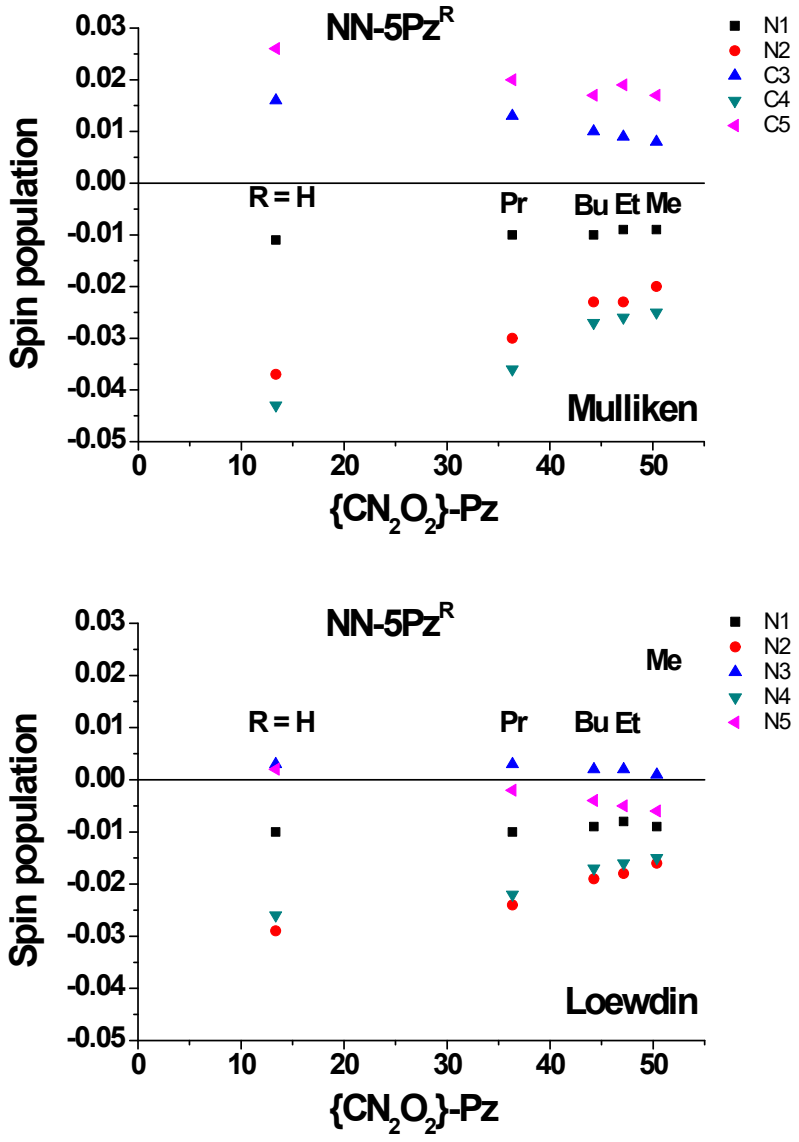

Fig. S17. The Mulliken (up) and Löwdin (down) atomic spin populations on Pz ring atoms of NN-5Pz^R radicals (at UB3LYP/def2-TZVP level) versus the {CN_2O_2}–Pz dihedral angle.

Table S24. Mulliken spin populations (UB3LYP) on selected atoms of NN-5Pz^{R} radicals, selected bond lengths (Å) and {CN_2O_2}–Pz dihedral angles (º).

		NN-5Pz^{H}			NN-5Pz^{Me}			NN-5Pz^{Et}			NN-5Pz^{nPr}			NN-5Pz^{nBu}		
	CCDC	WEHJUP			HIKJEQ			KIQXAL			KIRBEU			KIQWUE		
	Basis set: def2-	SVP	TZVP	QZVP	SVP	TZVP	QZVP	SVP	TZVP	QZVP	SVP	TZVP	QZVP	SVP	TZVP	QZVP
Pz	N(1)	–0.013	-0.011	–0.012	–0.009	–0.009	–0.010	–0.010	–0.009	–0.011	–0.012	-0.010	–0.012	–0.011	-0.010	–0.012
	N(2)	–0.039	-0.037	–0.036	0.021	–0.020	–0.020	–0.024	–0.023	–0.022	–0.028	-0.030	–0.030	–0.024	-0.023	–0.023
	C(3)	0.019	0.016	0.015	0.010	0.008	0.007	0.011	0.009	0.008	0.009	0.013	0.011	0.011	0.010	0.009
	C(4)	–0.050	-0.043	–0.041	–0.028	–0.025	–0.023	–0.029	–0.026	–0.024	–0.031	-0.036	–0.035	–0.031	-0.027	–0.026
	C(5)	0.045	0.026	0.029	0.034	0.017	0.021	0.036	0.019	0.021	0.020	0.020	0.026	0.037	0.017	0.022
NN	C_{NN}	–0.194	-0.164	–0.170	–0.225	–0.196	–0.200	–0.223	–0.193	–0.197	–0.163	-0.191	–0.197	–0.223	-0.191	–0.197
	N_{NO}	0.261-0.264	0.261-0.264	0.274-0.279	0.255-0.257	0.257-0.258	0.269	0.255-0.258	0.255-0.260	0.267-0.271	0.242-0.252	0.258-0.267	0.269-0.279	0.255-0.261	0.254-0.262	0.264-0.275
	O_{NO}	0.324-0.371	0.311-0.357	0.305-0.351	0.341-0.377	0.330-0.362	0.324-0.355	0.338-0.379	0.327-0.365	0.321-0.357	0.328-0.363	0.33-0.362	0.323-0.355	0.330-0.383	0.322-0.369	0.316-0.361
	C_{Me}(eq)	0.007-0.009	0.006-0.010	0.006-0.008	<0.001	<0.001	0.003	0.002	0.000-0.001	0.003	0.002	<0.002	0.003	0.001-0.002	<0.002	0.002-0.004
	C_{Me}(ax)	0.011-0.014	0.011-0.013	0.011-0.014	0.018	0.018-0.019	0.017-0.019	0.017-0.018	0.018-0.019	0.019	0.011-0.012	0.017-0.019	0.018-0.019	0.017-0.018	0.017-0.019	0.018
	N–O	1.279(3)			1.278(2), 1.279(2)			1.280(2), 1.281(2)			1.277(1), 1.278(1)			1.272(1), 1.288(1)		
	$C–N_{\{NN\}}$	1.325(3), 1.337(4)			1.340(2), 1.344(2)			1.340(2), 1.344(2)			1.349(2), 1.357(2)			1.338(2), 1.353(2)		
	{CN_2O_2}–Pz	13.36			50.36			47.14			36.35			44.26		

Table S25. Löwdin spin populations (UB3LYP) on selected atoms of NN-5Pz^{R} radicals.

		NN-5Pz^{H}			NN-5Pz^{Me}			NN-5Pz^{Et}			NN-5Pz^{nPr}			NN-5Pz^{nBu}		
	Basis set: def2-	SVP	TZVP	QZVP	SVP	TZVP	QZVP	SVP	TZVP	QZVP	SVP	TZVP	QZVP	SVP	TZVP	QZVP
Pz	N(1)	–0.012	–0.010	–0.008	–0.009	–0.007	–0.007	0.010	–0.008	–0.008	–0.012	–0.010	–0.010	–0.011	–0.009	–0.009
	N(2)	–0.035	–0.029	–0.027	–0.019	-0.016	–0.015	0.021	–0.018	–0.017	–0.028	–0.024	–0.022	–0.022	–0.019	–0.018
	C(3)	0.012	0.003	–0.001	-0.006	0.001	–0.001	0.007	0.002	–0.001	0.009	0.003	–0.001	0.007	0.002	–0.001
	C(4)	–0.038	–0.026	–0.018	–0.022	–0.015	–0.011	0.022	–0.016	–0.011	–0.031	–0.022	–0.016	–0.024	–0.017	–0.012
	C(5)	0.023	0.002	–0.006	0.013	–0.006	–0.013	0.014	–0.005	–0.012	0.020	–0.002	–0.010	0.015	–0.004	–0.011
NN	C_{NN}	–0.139	–0.061	–0.028	–0.163	-0.083	–0.049	0.161	–0.081	–0.048	–0.163	–0.083	–0.049	–0.161	–0.082	–0.048
	N_{NO}	0.246-0.251	0.222-0.230	0.204-0.214	0.240	0.216-0.221	0.199-0.206	0.239-0.244	0.214-0.224	0.198-0.208	0.242-0.252	0.218-0.231	0.201-0.215	0.238-0.246	0.213–0.227	0.196–0.211
	O_{NO}	0.314-0.359	0.291-0.333	0.288-0.329	0.329-0.365	0.308-0.337	0.304-0.332	0.327-0.367	0.305-0.339	0.301-0.335	0.328-0.363	0.307-0.337	0.303-0.332	0.320-0.370	0.300–0.343	0.296–0.338
	C_{Me}(eq)	0.006-0.008	0.005-0.006	0.004-0.05	<0.002	<0.001	<0.001	<0.002	<0.001	<0.001	0.002	0.001	0.001	0.002	0.001	<0.001
	C_{Me}(ax)	0.009-0.011	0.007-0.009	0.006-0.007	0.012	0.011	0.009	0.011-0.012	0.010-0.011	0.008-0.009	0.011-0.012	0.010-0.011	0.008–0.009	0.012	0.011	0.009

Literature referenced in the SI

1 W. L. F. Armarego, in *Purification of Laboratory Chemicals*, Elsevier, 2017, pp. 95–634.

2 L. Catala, K. Wurst, D. B. Amabilino and J. Veciana, Polymorphs of a pyrazole nitronyl nitroxide and its complexes with metal(ii) hexafluoroacetylacetonates, *J. Mater. Chem.*, 2006, **16**, 2736.

3 V. I. Ovcharenko, S. V Fokin, G. V Romanenko, Y. G. Shvedenkov, V. N. Ikorskii, E. V Tretyakov and S. F. Vasilevskii, Nonclassical Spin Transitions, *J. Struct. Chem.*, 2002, **43**, 153–167.

4 V. I. Ovcharenko, S. V. Fokin, G. V. Romanenko, V. N. Ikorskii, E. V. Tretyakov, S. F. Vasilevsky and R. Z. Sagdeev, Unusual spin transitions, *Mol. Phys.*, 2002, **100**, 1107–1115.

5 Y.-L. Gao, C. Tian, P. Gao, Y. Jiao, Y. Gong and X. Ma, Synthesis, crystal structures, and magnetic properties of nitroxide radical-coordinated manganese(II) and cobalt(II) complexes, *J. Chem. Res.*, 2021, **45**, 788–794.